Check for updates

ATM deficiency disrupts *Tcra* locus integrity and the maturation of $CD4^+CD8^+$ thymocytes

Irina R. Matei,[1,2] Rebecca A. Gladdy,[1,3] Lauryl M. J. Nutter,[1] Angelo Canty,[5] Cynthia J. Guidos,[1,4] and Jayne S. Danska[1,2,4]

[1]Program in Developmental and Stem Cell Biology, The Hospital for Sick Children Research Institute, University of Toronto, ON, Canada; [2]Department of Medical Biophysics, University of Toronto, ON, Canada; [3]Department of Surgery, University of Toronto, ON, Canada; [4]Department of Immunology, University of Toronto, ON, Canada; [5]Department of Mathematics and Statistics, McMaster University, Hamilton, ON, Canada

Mutations in *ATM* (ataxia-telangiectasia mutated) cause ataxia-telangiectasia (AT), a disease characterized by neurodegeneration, sterility, immunodeficiency, and T-cell leukemia. Defective ATM-mediated DNA damage responses underlie many aspects of the AT syndrome, but the basis for the immune deficiency has not been defined. ATM associates with DNA double-strand breaks (DSBs), and some evidence suggests that ATM may regulate V(D)J recombination. However, it remains unclear how ATM loss compromises lymphocyte development in vivo. Here, we show that T-cell receptor β (TCRβ)–dependent proliferation and production of $TCR\beta^{low}$ $CD4^+CD8^+$ (DP) thymocytes occurred normally in $Atm^{-/-}$ mice. In striking contrast, the postmitotic maturation of $TCR\beta^{low}$ DP precursors into $TCR\beta^{int}$ DP cells and $TCR\beta^{hi}$ mature thymocytes was profoundly impaired. Furthermore, $Atm^{-/-}$ thymocytes expressed abnormally low amounts of TCRα mRNA and protein. These defects were not attributable to the induction of a BCL-2–sensitive apoptotic pathway. Rather, they were associated with frequent biallelic loss of distal *Va* gene segments in DP thymocytes, revealing that ATM maintains *Tcra* locus integrity as it undergoes V(D)J recombination. Collectively, our data demonstrate that ATM loss increases the frequency of aberrant *Tcra* deletion events, which compromise DP thymocyte maturation and likely promote the generation of oncogenic TCR translocations. (Blood. 2007;109:1887-1896)

© 2007 by The American Society of Hematology

Introduction

Ataxia-telangiectasia (AT) is an autosomal recessive disease with a pleiotropic phenotype that includes cerebellar degeneration, immunodeficiency, sterility, radiosensitivity, and an elevated incidence of lymphoid malignancies.[1] AT is caused by mutations in *ATM*, a gene belonging to the phosphatidylinositol 3-kinase–related family of serine-threonine kinases that function in DNA damage surveillance and repair.[2] The radiosensitivity and increased cancer susceptibility of patients with AT and $Atm^{-/-}$ mice are thought to reflect loss of these ATM-dependent DNA damage responses,[2] whereas defective DNA repair by homologous recombination likely underlies the sterility of patients with AT.[3-5] However, the cause of AT-related immune deficiency has not been defined. Patients with AT are variably lymphopenic and display a range of cellular and humoral immunologic abnormalities,[6] leading to recurrent and sometimes fatal sinopulmonary infections. In particular, patients with AT exhibit low output of mature TCR^{hi} CD4 and CD8 single-positive (SP) thymocytes, and their peripheral T-cell pool often exhibits oligoclonal T-cell receptor (TCR) Vβ expansions and abnormally low naive/memory T-cell ratios.[7] Like patients with AT, *Atm*-deficient mice also have decreased numbers of mature thymocytes and peripheral T cells, suggesting defective intrathymic T-cell development.[8-11]

Given ATM's prominent role in regulating DNA damage responses, much interest has focused on the possibility that ATM has critical functions in V(D)J recombination, the somatic rearrangement process by which developing T and B lymphocytes generate a diverse repertoire of antigen receptor variable (*V*) genes. *Tcrb* and *Tcra* recombination occur sequentially during the successive CD4/CD8 double-negative (DN) and CD4/CD8 double-positive (DP) stages of T-cell development, respectively. Signaling through TCRβ-containing pre-TCR complexes is required to generate a large pool of DP thymoctyes from DN precursors. *Tcra* rearrangement begins in postmitotic DP thymocytes.[12] However, the *Tcra* locus can undergo successive rounds of secondary recombination to maximize the opportunity for DPs to produce a TCRαβ heterodimer that can induce positive selection in response to self major histocompatibility complex proteins.[13-15] Thus, failure to make successful (in-frame) *Tcrb* rearrangements arrests T-cell development at the DN stage, whereas failure to produce an appropriate (selectable) *Tcra* rearrangement arrests development at the DP stage. $Atm^{-/-}$ mice express T-cell receptors and exhibit only partial deficits in the size of their immature DP and mature SP thymocyte pools,[8-11] indicating that ATM is not essential for recombination of *Tcrb* or *Tcra* loci.

V(D)J recombination is initiated by the lymphocyte-specific RAG-1/2 endonuclease, which generates DNA double strand breaks (DSBs) in between recombination signal sequences and adjacent antigen receptor variable (*V*), diversity (*D*), or joining (*J*) gene segments.[16] The resulting coding ends (CEs) and signal ends (SEs) are repaired by the nonhomologous end-joining (NHEJ) complex to make coding joints (CJs) and signal joints (SJs), respectively. Defective NHEJ causes abnormal accumulation of CEs[17] and induction of p53-dependent apoptosis in thymocytes.[18] In NHEJ-p53 double-mutant mice, defective DSB repair during

Submitted May 3, 2006; accepted October 19, 2006. Prepublished online as *Blood* First Edition Paper, October 31, 2006; DOI 10.1182/blood-2006-05-020917.

The online version of this article contains a data supplement.

The publication costs of this article were defrayed in part by page charge payment. Therefore, and solely to indicate this fact, this article is hereby marked "advertisement" in accordance with 18 USC section 1734.

© 2007 by The American Society of Hematology

Downloaded from http://ashpublications.net/blood/article-pdf/109/5/1887/1478507/zh800507001887.pdf by guest on 08 June 2024

IgH recombination causes frequent deletion of telomeric *VH* gene segments, facilitating generation of oncogenic translocations with *cMyc* and initiating *IgH/cMyc* amplification through repeated cycles of bridge-breakage-fusion.[19-21] Thus, defective NHEJ of RAG-induced DSBs can promote lymphoid leukemogenesis.

Interestingly, ATM localizes to V(D)J recombination-induced DSBs,[22] suggesting that it may monitor recombination intermediates, thus limiting the oncogenic consequences of aberrant V(D)J recombination. Furthermore, 2 ATM substrates, H2AX and NBS1, also localize to V(D)J-induced DSBs, and inactivating mutations in these proteins cause a phenotype reminiscent of ATM deficiency.[23-25] Although NHEJ of recombining *Tcr* loci does not appear to be profoundly defective in ATM-deficient thymocytes, several observations suggest that ATM-deficient T-cell precursors recombine *Tcr* loci with poor fidelity. T-cell leukemias arising in patients with AT and $Atm^{-/-}$ mice frequently harbor chromosomal translocations involving *Tcr* and *Ig* genes.[1,26] In addition, peripheral blood lymphocytes from patients with AT display frequent abnormal *trans*-rearrangements of *TCR* loci,[27] a defect also seen in NHEJ-deficient T-cell precursors.[28]

Finally, a recent study showed that $Atm^{-/-}$ T- and B-cell precursors display a 50% reduction in normal CJs and a high frequency of abnormal "hybrid" joins between SEs and CEs when rearrangement occurs by inversion, but not deletion.[29] During deletional recombination, CJs are made on chromosomes, whereas SJs are joined on extrachromasomal circles that are subsequently lost from the cells. In contrast, inversional recombination requires that both the CJs and SJs be made on the same chromosome. Thus, ATM might be particularly important in stabilizing DSB repair complexes during the more demanding process of inversional V(D)J recombination. However, because most *Tcrb* and *Tcra* rearrangements occur by deletional recombination,[30] it is not clear whether defects in ATM-induced DSB stabilization can explain the impaired T-cell development observed in ATM-deficient patients and mice.

Here, we address 2 key questions regarding ATM function. Does the T-cell deficiency in $Atm^{-/-}$ mice result from inefficient V(D)J recombination at *Tcr* loci? Alternatively, does loss of ATM-induced DNA damage checkpoints impair proliferation and/or survival of developing thymocytes? We show that *Tcrb* recombination was not obviously impaired in $Atm^{-/-}$ thymocytes, enabling the production of a normal-sized pool of $TCR\beta^{low}$ DP thymocytes in response to pre-TCR signals. In striking contrast, the postmitotic generation of $Atm^{-/-}$ $TCR\beta^{int}$ DP thymocytes and their $TCR\beta^{hi}$ SP progeny was profoundly impaired; neither defect was rescued by BCL-2 overexpression. Although we did not observe *Tcra* CE accumulation, the hallmark of defective NHEJ, $Atm^{-/-}$ thymocytes expressed dramatically reduced levels of TCRα mRNA and protein. Moreover, cytogenetic analyses revealed frequent biallelic loss of a large chromosomal region encoding the most telomeric *Va* gene segments. Thus, our findings reveal that ATM loss compromises the fidelity of *Tcra* locus recombination in DP thymocytes, decreasing the pool of $TCR\beta^{int}$ DP precursors available for positive selection into the mature CD4 or CD8 lineages.

Materials and methods

Mice

129/SvEv-Atm^{tm1Awb} heterozygous mice[8] (Jackson Laboratory, Bar Harbor, ME) were bred in our specific pathogen facility (Hospital for Sick Children, Toronto, ON, Canada) to generate $Atm^{+/+}$, $Atm^{+/-}$, and $Atm^{-/-}$ progeny. *Atm* genotypes were determined by polymerase chain reaction (PCR) amplification of tail DNA, using the following primers: *Atm*-wt antisense, 5′-TCCGAATTTGCAGGAGTTG-3′; *Atm*-wt sense, 5′-GCTGCCATACTTGATCCATG-3′; neomycin antisense, 5′-AGGTGAGATGACAGGAGATC-3′; neomycin sense, 5′-CTTGGGTGGAGAGGCTATTC-3′. To generate $Atm^{-/-}$;*Bcl2* Tg^{+} mice, *Bcl2* Tg^{+} mice obtained from Dr Korsmeyer (Sentman et al[31]) were bred to 129/SvEv-Atm^{tm1Awb} heterozygous mice. $Atm^{+/-}$;*Bcl2* Tg^{+} mice were backcrossed to 129/SvEv-Atm^{tm1Awb} heterozygous mice to generate the genotypes of interest. The presence of the *lckpr-BCL2* transgene was determined by genomic DNA PCR amplification for 30 cycles using the following primers: *GH* (human growth hormone) sense, 5′-GTAGCCATTGCAGCTAGGTG-3′, and *BCL2 Tg* antisense, 5′-CTTTGTGGAACTGTACGGCCCCAGCATGCG-3′, at a final concentration of 1 μM each. *BCL2* transgene expression was confirmed by intracellular staining with anti–hBCL-2-PE (6C8; BD Biosciences, San Jose, CA). Three- to 4-week-old $Atm^{-/-}$ mice and $Atm^{+/+}$ littermates or age-matched controls were used in all experiments, unless otherwise indicated. All animal experiments followed protocols approved by the Hospital for Sick Children Animal Care Committee (Toronto, ON, Canada).

Antibodies and flow cytometry

Antibodies used in this study were anti-CD8α (YTS-169.4), -CD4 (RM4-5), -TCRβ (H57-597), -TCRα (H28-710), -CD5 (53-7.3), -CD69 (H1.2F3), rat IgG2a, IgG2b, and Armenian hamster IgG. Antibody-fluorochrome conjugates and avidin second-stage reagents were purchased from BD Biosciences, eBiosciences (San Diego, CA), or produced in our laboratory using standard techniques and used at predetermined saturating concentrations. Sorting of DP cells was performed on a DakoCytomation MoFlow. Data acquired on FACS Calibur or DakoCytomation cytometers was imported into either CellQuest (Becton Dickinson, Franklin Lakes, NJ) or FlowJo (Tree Star, Ashland, OR) software for analysis. Dead cells were excluded from analysis based on low forward scatter and high propidium iodide staining.

Intracellular staining

The levels of intracellular TCRβ were assessed by flow cytometry using anti–TCRβ-APC (H57-597) or control biotinylated hamster IgG isotype followed by SAv-APC. Thymocytes were surface-stained with anti–CD4-PE and anti–CD8-FITC, fixed, permeabilized, and stained intracellularly using the BD Cytofix/Cytoperm Kit (BD Biosciences) as per the manufacturer's instructions.

Western blotting/immunoprecipitation

TCRα protein was detected with hamster anti–mouse TCRα constant chain (clone H28-710) in postnuclear extracts prepared as previously described[32] except dithiothreitol was omitted to preserve integrity of the TCRαβ heterodimer. Densitometry was performed using the FluorChem imaging system and software (Alpha Innotech, San Leandro, CA) and standardized with an anti–β-actin (clone AC-15) loading control. Immunoprecipitation was performed using CNBr sepharose (Amersham Biosciences, Piscataway, NJ) coupled to anti-TCRβ (H57-597) or isotype IgG control antibodies according to the manufacturer's protocol. Immunoprecipitates were Western blotted and examined with purified anti-TCRα antibody. Primary antibodies were detected with protein A (Amersham Biosciences) or anti–mouse IgG (Jackson ImmunoResearch Laboratories, West Grove, PA) coupled to horseradish peroxidase followed by enhanced chemiluminescence per manufacturer's instructions (Amersham Biosciences).

In vitro maturation of DP thymocytes

Three million $Atm^{-/-}$ or littermate $Atm^{+/+}$ thymocytes were cultured in 6-well plates precoated with 7.5 μg/mL purified anti-TCRβ (H57-597) or hamster IgG isotype control (Caltag, San Francisco, CA), as previously described.[33]

BrdU assays

Four- to 8-week-old $Atm^{-/-}$ or $Atm^{-/-}$;*Bcl2* Tg^{+} mice and age-matched controls received 2 intraperitoneal injections of 5-bromo-2′deoxyuridine

Downloaded from http://ashpublications.net/blood/article-pdf/109/5/1887/1478507/zh800507001887.pdf by guest on 08 June 2024

(BrdU; 1 mg each, 4 hours apart) at day 0. Thymocytes were isolated 1 to 5 days after injection and stained as described in "Antibodies and flow cytometry." BrdU detection was performed using the BrdU Flow Kit per the manufacturer's instructions (BD Biosciences).

Results

Atm$^{-/-}$ DP thymocytes express abnormally low levels of surface TCR

To investigate possible functions of ATM in T-cell development, we examined the steady state phenotype and number of thymocytes in *Atm*$^{-/-}$ mice compared with *Atm*$^{+/-}$ and *Atm*$^{+/+}$ littermates from 5 to 60 days of age. Consistent with prior reports, we observed a 40% to 60% decrease in thymic cellularity of *Atm*$^{-/-}$ mice.[3,8] In particular, the frequencies and absolute numbers of mature CD4$^+$ and CD8$^+$ thymocyte populations were severely decreased in *Atm*$^{-/-}$ mice relative to littermate controls (Figure 1A,C). Because production of mature SP thymocytes requires expression of TCRαβ in DP precursors, we examined surface TCRβ expression on *Atm*$^{-/-}$ DP thymocytes (Figure 1B-C). As expected, most *Atm*$^{+/+}$ DP thymocytes expressed intermediate levels of TCRβ. However, as previously noted,[10,11] most *Atm*$^{-/-}$ DP thymocytes were TCRβ^{low} (Figure 1B-C). The ratio of TCRβ^{low} to TCRβ^{int} DP thymocytes in wild-type mice was approximately 1:2, compared with 4:1 in *Atm*$^{-/-}$ mice, reflecting a reduction in both the percentage and absolute number of TCRβ^{int} DP thymocytes (Figure 1C). However, the small pool of SP thymocytes in *Atm*$^{-/-}$ mice displayed normal TCRβ surface expression, suggesting a stage-specific defect in TCRαβ production.

We next examined the capacity of *Atm*$^{-/-}$ DP thymocytes to respond to TCR engagement in vitro. Plate-bound anti-TCRβ antibody was used to engage the TCR in short-term DP thymocyte cultures. As previously reported,[34] within 24 hours most wild-type DP thymocytes responded to TCR signaling by down-regulating CD4 and CD8 coreceptors and up-regulating CD5 and CD69 (Figure 1D). In contrast, less than 30% of the *Atm*$^{-/-}$ DP thymocytes responded in a similar manner, suggesting that few express sufficient surface TCRαβ to initiate positive selection.

ATM loss compromises postmitotic generation of TCRβ^{int} DP and TCRβ^{hi} SP thymocytes

The most striking consequence of ATM loss on T-cell development is the reduction in TCRβ^{int} DP thymocytes and their TCRβ^{hi} progeny (Figure 1). TCRβ^{int} DP thymocytes are postmitotic, harbor in-frame TCRβ rearrangements, and are actively recombining their *Tcra* loci.[13] These cells are generated from precursors that cycle extensively during the DN3 to DP transition.[35] We reasoned that the reduction in *Atm*$^{-/-}$ TCRβ^{int} DP thymocytes could reflect a defect in pre–TCR-induced clonal expansion of DN precursors or reduced survival of postmitotic DP thymocytes. To distinguish between these alternatives, we monitored the initial generation and subsequent maturation of *Atm*$^{-/-}$ DP thymocytes 1 to 5 days after BrdU pulse labeling in vivo. As expected from previous reports,[36] most labeled wild-type cells were TCRβ^{low} DP precursors 1 day after BrdU injection, and their numbers decreased dramatically over the next 5 days, as they either died or matured into SP thymocytes (Figure 2A-B). Similar proportions of the DN and DP subsets were labeled in *Atm*$^{-/-}$ and *Atm*$^{+/+}$ controls on day 1, demonstrating that ATM loss did not affect thymocyte proliferation or the initial generation of TCRβ^{low} DP thymocytes (Figure 2A-B).

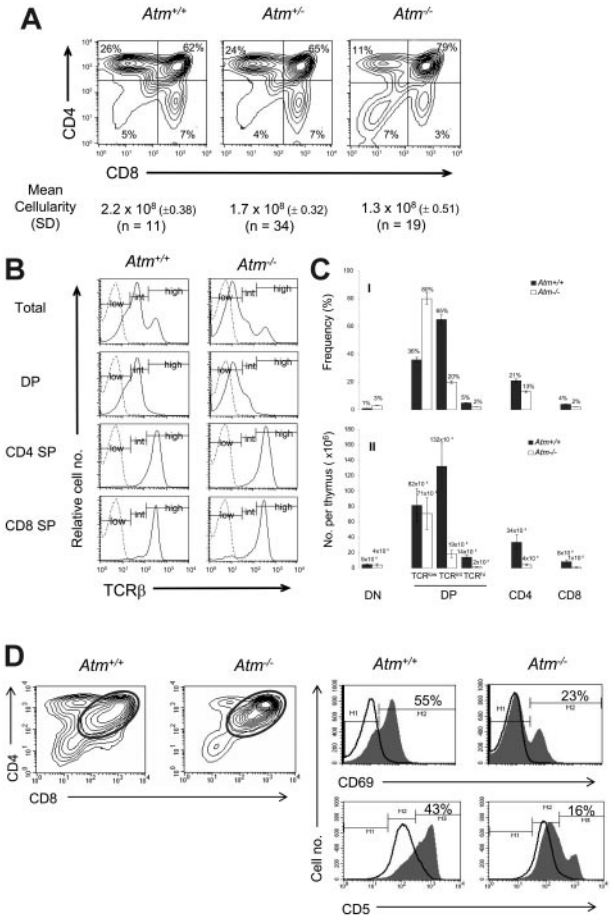

Figure 1. ATM deficiency leads to a severe deficit in TCRβ^{int} and TCRβ^{hi} thymocytes and diminished responses to TCR engagement in vitro. (A) Frequency of SP thymocytes in *Atm*$^{-/-}$, *Atm*$^{+/-}$, and *Atm*$^{+/+}$ mice. Flow cytometric analysis of T-cell development was performed in 3- to 4-week-old mice segregating the ATM mutant allele. Thymocytes were stained with anti–CD4–phycoerithryn (PE), anti–CD8–fluorescein isothyocyanate (FITC), and anti–TCRβ-biotin, revealed with streptavidin-allophycocyanin (SAv-APC). Representative CD4 versus CD8 staining profiles of each genotype are shown, together with the quadrant gates used to identify DN, DP, and SP thymocytes. (B) TCRβ expression on thymocyte subsets from *Atm*$^{-/-}$ and *Atm*$^{+/+}$ mice. TCRβ levels (solid) are compared with staining of isotype-matched control antibodies (dashed). (C) Percentages and absolute numbers of thymocyte subsets in *Atm*$^{-/-}$ mice and littermates. The bar graphs depict percentages (i) and absolute numbers (ii) of DN, DP (TCRβ^{low}, TCRβ^{int}, and TCRβ^{hi}) and CD4 or CD8 SP thymocytes in *Atm*$^{-/-}$ mice (□) and littermates (■). The numbers above each bar represent the mean. The graphs display the mean ± SD for 9 *Atm*$^{+/+}$ and 12 *Atm*$^{-/-}$ mice. Percentages and absolute numbers of CD8$^+$ SP cells were determined by gating on TCRβ^{hi} CD8$^+$ SP cells to eliminate immature single-positive cells. All differences were statistically significant ($P < .001$ by Student *t* test) except for the DN frequency, DN, and TCRβ^{low} DP absolute number comparisons. (D) CD4 versus CD8 expression on thymocytes from 3-week-old *Atm*$^{+/+}$ or *Atm*$^{-/-}$ mice was assessed after overnight culture in the presence of plate-bound anti-TCRβ antibody. Fluorescence signals were gated to display CD69 or CD5 staining on CD4$^+$CD8$^+$ DP thymocytes. Expression of the early activation markers CD69 and CD5 by DP thymocytes from *Atm*$^{-/-}$ mice and littermate controls was evaluated by flow cytometry after overnight culture in the presence (shaded) or absence (open) of stimulation with anti-TCRβ.

Most labeled wild-type DP thymocytes became TCRβ^{int} by day 3. In striking contrast, the postmitotic generation of TCRβ^{int} DP thymocytes was highly inefficient in *Atm*$^{-/-}$ mice. The conversion of *Atm*$^{-/-}$ TCRβ^{int} DP into TCRβ^{hi} SP cells was also less efficient than in *Atm*$^{+/+}$ controls (most evident at day 5 after labeling). Therefore, normal numbers of *Atm*$^{-/-}$ TCRβ^{low} DP thymocytes were produced, but their postmitotic conversion into TCRα-expressing TCRβ^{int} DP and mature TCRβ^{hi} SP thymocytes was seriously impaired. This loss most likely reflects a survival defect,

Downloaded from http://ashpublications.net/blood/article-pdf/109/5/1887/1478507/zh800507001887.pdf by guest on 08 June 2024

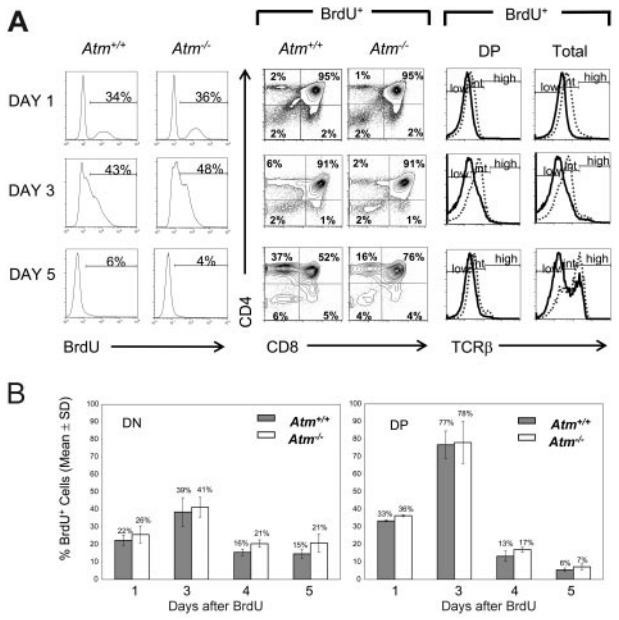

Figure 2. Impaired production of TCRβ^{int} and TCRβ^{hi} thymocytes in *Atm*$^{-/-}$ mice. (A) BrdU labeling of total thymocytes from *Atm*$^{-/-}$ mice and age-matched *Atm*$^{+/+}$ controls at indicated time points after BrdU injection (histograms, left). Middle panels depict CD4 versus CD8 thymocyte profiles of *Atm*$^{-/-}$ and *Atm*$^{+/+}$ mice gated on BrdU^{+} cells at days 1, 3, and 5 after injection. TCRβ profiles (right) are shown for *Atm*$^{+/+}$ (dotted) and *Atm*$^{-/-}$ (solid) thymocytes gated on BrdU^{+} DP and total thymocytes. (B) Proportions of BrdU^{+} DN and DP thymocyte populations in *Atm*$^{-/-}$ mice after pulse labeling. The graphs represent the mean percentage (±SD) of BrdU^{+} cells within the DN (left) and DP (right) thymocyte subsets from *Atm*$^{-/-}$ mice compared with age-matched controls. Results are representative of 2 to 3 experiments per time point, with analysis of 2 to 3 animals of each genotype per experiment.

because we observed a statistically significant 2-fold increase in the numbers of cells expressing active caspase-3 in the cortex of *Atm*$^{-/-}$ thymi where DP cells reside, but no genotype-dependent variation in the medulla (Figure S1, available on the *Blood* website; see the Supplemental Materials link at the top of the online article). Rapid clearance of apoptotic thymocytes by resident macrophages[37] likely prevented further accumulation of caspase-3–positive cells in *Atm*$^{-/-}$ thymic lobes. Collectively, these observations reveal that ATM deficiency does not impair pre–TCR-dependent proliferation during the DN to DP transition. Rather, ATM loss impairs survival during the postmitotic conversion of TCRβ^{low} DP into TCRβ^{int} DP thymocytes.

ATM regulates postmitotic DP thymocyte survival by a BCL-2–independent pathway

Members of the BCL-2 family regulate thymocyte survival, and RORγ-dependent expression of BCL-X_L supports DP thymocyte survival during secondary *Tcra* recombination.[38] Therefore, we next asked whether the postmitotic survival defect of TCRβ^{int} DP thymocytes could be rescued by expression of a human *Bcl2* transgene driven by the *Lck* proximal promoter. Intracellular BCL-2 staining confirmed transgene expression in all thymocyte subsets of *Atm*$^{-/-}$*;Bcl2 Tg*$^{+}$ mice (data not shown). The *Bcl2* transgene reduced the numbers of caspase-3^{+} apoptotic cells in both *Atm*$^{+/+}$ and *Atm*$^{-/-}$ thymi (data not shown) and slightly increased the absolute numbers of most thymocyte subsets in *Atm*$^{-/-}$ mice (Figure S2). However, the numbers of TCRβ^{int} DP and TCRβ^{hi} SP thymocytes in *Atm*$^{-/-}$*;Bcl2 Tg*$^{+}$ mice remained significantly lower than those in either Tg^{+} or Tg^{-} *Atm*$^{+/+}$ mice (Figure S2). BrdU pulse-chase experiments showed that BCL-2 overexpression in *Atm*$^{-/-}$ mice failed to rescue postmitotic production of TCRβ^{int} DP thymocytes to wild-type levels (Figure 3). On the basis of these experiments we concluded that ATM loss does not compromise generation of TCRβ^{int} DP thymocytes by activating a BCL-2–sensitive apoptotic pathway.

Atm$^{-/-}$ thymocytes express a diverse *Tcrb* repertoire

To determine the basis for the decrease in the TCRβ^{int} DP thymocyte population, we examined intracellular TCRβ (TCRβic) protein expression. TCRβic protein levels were equivalent in *Atm*$^{-/-}$ and *Atm*$^{+/+}$ DP thymocytes (Figure 4A), suggesting that defects in TCRβ rearrangement or expression did not account for the reduction in the TCRβ^{int} DP population. However, we reasoned that inefficient V(D)J recombination might limit TCRβ chain diversity. Therefore, we carried out complementarity-determining region 3 (CDR3) length analysis to examine the junctional diversity of TCRβ transcripts in *Atm*$^{-/-}$ thymocytes. The CDR3 region is created by V(D)J coding end modifications and greatly contributes to TCRβ clonal diversity. Thymocyte cDNA samples from *Atm*$^{-/-}$ mice and controls were PCR-amplified with primers specific for 1 of 2 widely used *Vb* gene segments (*Vb1* or *Vb8*), together with an antisense *Cb* primer. As expected, we obtained a Gaussian distribution of discrete 3-bp (base pair) spaced CDR3 lengths representing in-frame transcripts in wild-type thymocytes (Figure 4B). The CDR3 region length distribution of *Atm*$^{-/-}$

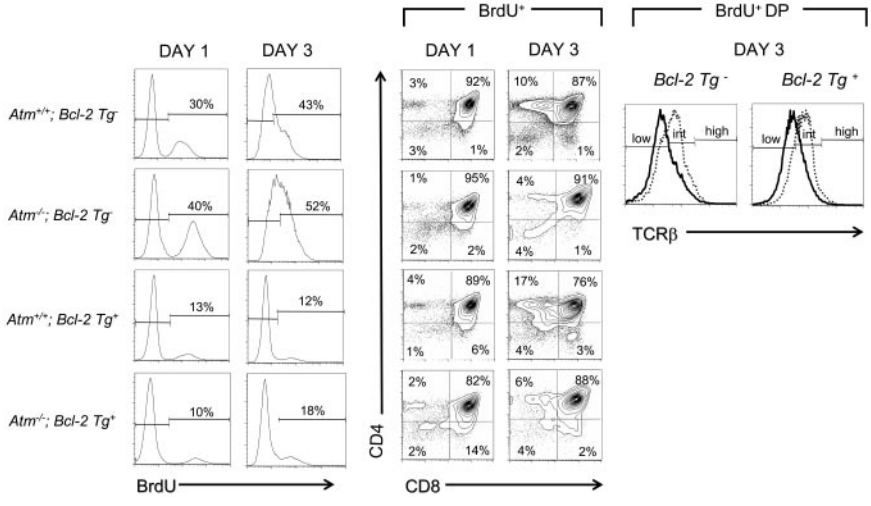

Figure 3. BCL-2 overexpression fails to rescue the generation of TCRβ^{int} thymocytes in ATM-deficient mice. BrdU labeling of total thymocytes from *Atm*$^{-/-}$ and *Atm*$^{+/+}$ mice segregating the *Bcl2* transgene at indicated time points after BrdU injection (histograms, left). CD4 versus CD8 thymocyte profiles (left) gated on BrdU^{+} cells are displayed at 1 or 3 days after injection in *Atm*$^{-/-}$ and *Atm*$^{+/+}$ mice segregating the *Bcl2* transgene. TCRβ profiles (right) gated on BrdU^{+} cells are shown for DP thymocytes from *Atm*$^{-/-}$ (solid) and *Atm*$^{+/+}$ (dotted) mice segregating the *Bcl2* transgene, 3 days after BrdU injection. Results are representative of 2 experiments per time point, with 2 to 3 animals of each genotype.

Downloaded from http://ashpublications.net/blood/article-pdf/109/5/1887/1478507/zh800507001887.pdf by guest on 08 June 2024

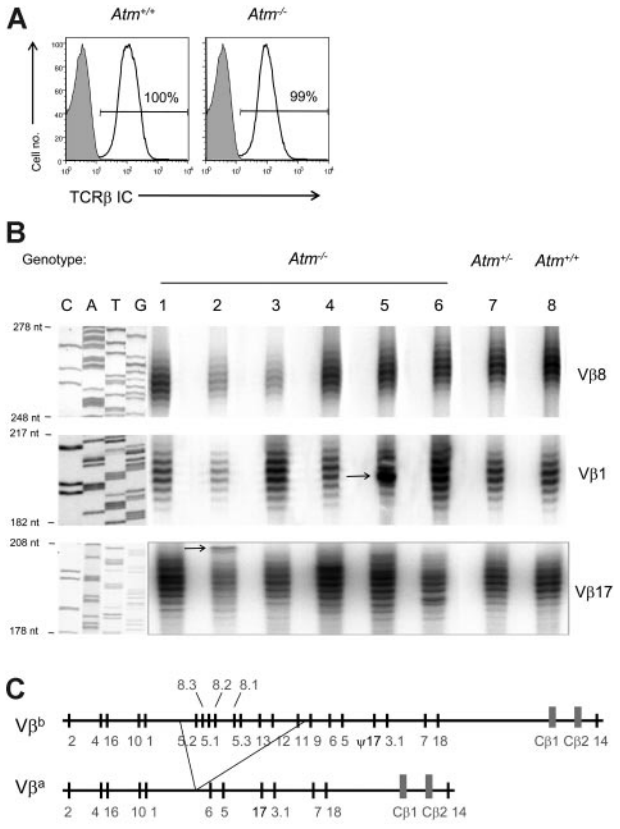

Figure 4. *Atm*$^{-/-}$ thymocytes express *Tcrb* transcripts of unrestricted diversity. (A) Normal levels of TCRβic in ATM-deficient CD4^{+}CD8^{+} DP thymocytes. (B) Diverse CDR3 length of selectable *(Vb1, Vb8)* or nonselectable *(Vb17) Tcrb* transcripts in individual *Atm*$^{-/-}$, *Atm*$^{+/-}$, and *Atm*$^{+/+}$ thymi. For *Vb1* the arrow indicates a dominant clonal rearrangement in one *Atm*$^{-/-}$ animal, probably a preleukemic clonal expansion. (C) Schematic representation of the *Vb*^{a} and *Vb*^{b} haplotypes (the former contains a deletion of approximately half of the *Vb* gene segments and a functional *Vb17* gene, whereas the latter contains the *Vb17* pseudogene, *ψ17*).[40] For *Vb17*, the arrow indicates a rearrangement that falls out of the normal CDR3 length distribution.

thymocytes was comparable to *Atm*$^{+/-}$ and *Atm*$^{+/+}$ controls. However, a dominant *Vb1* CDR3 length was detected in one 3-week-old *Atm*$^{-/-}$ animal (Figure 4B, arrow), possibly an early manifestation of the pre–T-cell lymphoblastic leukemia/lymphoma characteristic of murine ATM deficiency.[8,39]

To exclude the possibility that robust pre–TCR-induced clonal expansion obscured a subtle defect in V(D)J recombination, we examined transcripts from the *Vb17* pseudogene which cannot produce a functional TCRβ chain in mice carrying the *Vb* haplotype (Figure 4B-C).[40] Even in the absence of selection for in-frame transcripts, Vβ17 transcripts displayed CDR3 lengths that were similarly diverse in *Atm*$^{-/-}$ and control thymocytes (Figure 4B). Finally, we used a panel of Vβ-specific monoclonal antibodies to examine the diversity of TCRβ proteins expressed on the surface of TCRβ^{hi} ATM-deficient thymocytes. We found that *Atm*$^{-/-}$ and control mature thymocytes exhibited similar frequencies of TCR-Vβ3, 5, 6, 7, 8, 9, 10, 11, 12, and 13 (data not shown). Therefore, *Atm*$^{-/-}$ and wild-type thymocytes express an equally diverse TCRβ repertoire, suggesting that ATM loss does not limit *Vb* gene segment use or junctional diversity during *Tcrb* recombination.

Reduced TCRα expression in *Atm*$^{-/-}$ thymocytes

TCRα expression is limiting for the assembly of TCRαβ complexes in DP thymocytes,[41] and we observed normal intracellular TCRβ expression in DP thymocytes (Figure 4A). Therefore, we examined TCRαβ heterodimer expression in mutant versus wild-type thymocytes. Western blot analysis revealed an 8-fold reduction in the amount of TCRαβ heterodimer in *Atm*$^{-/-}$ thymocytes (Figure 5A). Immunoprecipitation experiments also revealed extremely low levels of TCRαβ heterodimers in *Atm*$^{-/-}$ thymocytes compared with littermate controls (Figure 5B). Quantification of TCRα transcripts in *Atm*$^{-/-}$ versus *Atm*$^{+/+}$ thymocytes identified a 3- to 7-fold reduction in abundance (Figure 5C), confirming that decreased TCRα protein levels reflected reduced amounts of steady-state transcripts.

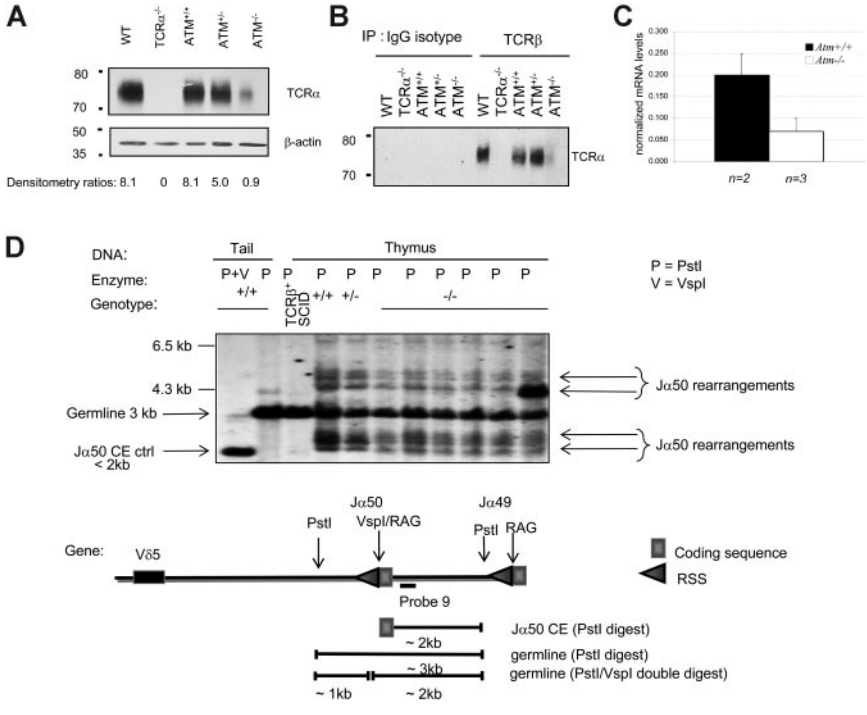

Figure 5. Analysis of TCRα expression and *Ja50* recombination in ATM-deficient thymocytes. (A) Western blot analysis using anti-TCRα performed on thymocyte postnuclear extracts from mice segregating the *Atm* mutation, wild-type C57BL/6, and *Tcra*$^{-/-}$ controls. Reprobing with anti–β-actin verified equal loading. The numbers below each lane represent densitometric quantification of the relative amount of TCRα compared with the loading control. (B) Total thymocyte postnuclear extracts from the indicated mouse strains were immunoprecipitated with anti-TCRβ (H57-597) or hamster IgG isotype control antibodies and resolved by sodium dodecyl sulfate–polyacrylamide gel electrophoresis (SDS-PAGE) under nonreducing conditions. Western blot analysis was performed with anti-TCRα. (C) Quantitative reverse transcriptase (RT)–PCR of TCRαC transcripts in thymocytes from *Atm*$^{+/+}$ (■) and *Atm*$^{-/-}$ (□) mice. The graph depicts the mean ± SD measurements for 2 individual *Atm*$^{+/+}$ and 3 individual *Atm*$^{-/-}$ mice. (D) *Ja50* rearrangements but not unrepaired CEs can be detected in *Atm*$^{-/-}$ thymocytes. In one 12-week-old *Atm*$^{-/-}$ animal, we observed expansion of a clone that had already undergone *Tcra* rearrangement (last lane). A restriction map of the 5′ end of the *Tcra* locus indicates the expected sizes of the products generated by digestion at the relevant restriction enzyme sites.

Downloaded from http://ashpublications.net/blood/article-pdf/109/5/1887/1478507/zh800507001887.pdf by guest on 08 June 2024

To determine whether impaired *Tcra* recombination could account for decreased *Tcra* expression in *Atm*$^{-/-}$ thymocytes, we analyzed *Tcra* recombination intermediates and end products by Southern blotting. We first used a strategy that detects rearrangements and abnormally persisting CEs at *Ja50* and *Ja49*, the most 5′ *Va*-proximal segments of the *Ja* cluster. These segments are preferentially involved in the initiation of *Tcra* rearrangement,[42] and defective NHEJ causes abnormal CE persistence in this proximal region.[43] In contrast to *Tcrb*-transgenic *Prkdc*$^{scid/scid}$ thymocytes,[43] we observed similar levels of *Ja50* rearrangements in *Atm*$^{-/-}$ and wild-type thymocytes (Figure 5D). Furthermore, we did not detect accumulation of *Ja50* CEs in *Atm*$^{-/-}$ thymocytes. Using a different Southern blot strategy to examine *Ja50* and *Ja49* SE intermediates and SJ recombination products, we found that SEs were precisely rejoined into SJs in *Atm*$^{-/-}$ and control thymocytes (Figure S3). In addition, the abundance of *Ja50* and *Ja49* SEs or SJs was similar in the 2 *Atm* genotypes (Figure S3). These strategies have previously revealed profound impairment of proximal *Ja* rearrangement and accumulation of proximal *Ja* CEs[43] in NHEJ-deficient mice. We did not find similar defects in the initiation or processing of proximal *Ja* recombination intermediates in *Atm*$^{-/-}$ thymocytes. Therefore, if ATM loss impairs NHEJ during *Tcra* recombination, it was not detected by these approaches.

Analysis of secondary *Tcra* recombination in *Atm*$^{-/-}$ thymocytes

We next examined whether secondary *Tcra* recombination is impaired in *Atm*$^{-/-}$ thymocytes by a Southern blot strategy predicated on the observation that secondary *Tcra* rearrangements cause deletion of 5′ *Ja* segments proximal to the *Va* cluster.[13,14] Using probes specific for proximal 5′, "middle," and distal 3′ regions of the *Ja* cluster, we found equivalent deletion of the proximal and middle *Ja* chromosomal regions in *Atm*-deficient and wild-type thymocytes, consistent with a similar extent of secondary *Tcra* recombination (Figure 6A). To further assess *Ja* usage, we sequenced 30 independent *Va3-Ca* transcripts isolated from *Atm*$^{-/-}$ and littermate control thymi. These sequences also revealed similar distributions of proximal, middle, and distal *Ja* segments in *Atm*$^{-/-}$ and wild-type Vα3-Cα transcripts (Figure 6B). Thus, we saw no bias in *Ja* usage that would reflect impaired secondary *Tcra* recombination in the absence of ATM.

Biallelic deletions of distal *Va* gene segments in *Atm*$^{-/-}$ thymocytes

Although we observed similar levels of proximal, middle, and distal *Ja* rearrangements in *Atm*$^{-/-}$ thymocytes, our strategy could not distinguish between normal rearrangements involving *Va* gene segments and aberrant rearrangements involving other chromosomal regions. A hallmark of the T-cell leukemias characteristic of both human and murine ATM deficiency is recurrent abnormalities involving the *Tcra* locus on chromosome 14,[26,44] often resulting in loss of *Tcra* locus material.[26] These considerations prompted us to investigate *Tcra* locus integrity using molecular cytogenetics. Because DP thymocytes undergoing *Tcra* rearrangement are postmitotic cells, we performed interphase fluorescent in situ hybridization (iFISH) experiments to assess the integrity of the *Tcra* locus in primary total and purified DP thymocytes isolated from 4-week-old *Atm*$^{-/-}$ and *Atm*$^{+/+}$ mice. The murine *TcraC* region is separated from the most 5′ distal end of *TcraV* gene cluster on chromosome 14 by about 1.3 megabases.[30] In addition, deletional *Tcra* recombination progresses from proximal to distal *Va* segments. Therefore, we selected BAC probes containing the *TcraC* locus and 6 of the most distal *TcraV* regions, to ensure maximal sensitivity in detecting abnormalities.

iFISH signals from *TcraC* and *TcraV* probes were analyzed in unfractionated and in sorted DP thymocyte samples isolated from *Atm*$^{+/+}$ and *Atm*$^{-/-}$ mice (Figure 7; Table 1; Tables S1, S2; Figure S4). The signal distributions in thymocytes from individual mice are shown in Figure 7, and the pooled signal distributions from mutant compared with wild-type thymocytes are shown in Table 1, Table S1, and Table S2. A standard chi-square test of the iFISH signal distributions revealed significant differences in the distribution of *TcraC* and *TcraV* signals between *Atm* genotypes (Tables S1, S2), so we carried out additional comparisons of genotype-specific differences in *Tcra* locus signals.

One major difference was that compared with wild-type cells, fewer mutant thymocytes had 2 *TcraC* signals per cell (Figure 7A; $P < .001$; Table 1) and a greater number had more than 2 *TcraC* signals per cell (Figure 7B; $P < .001$; Table 1). We noted a second striking difference in

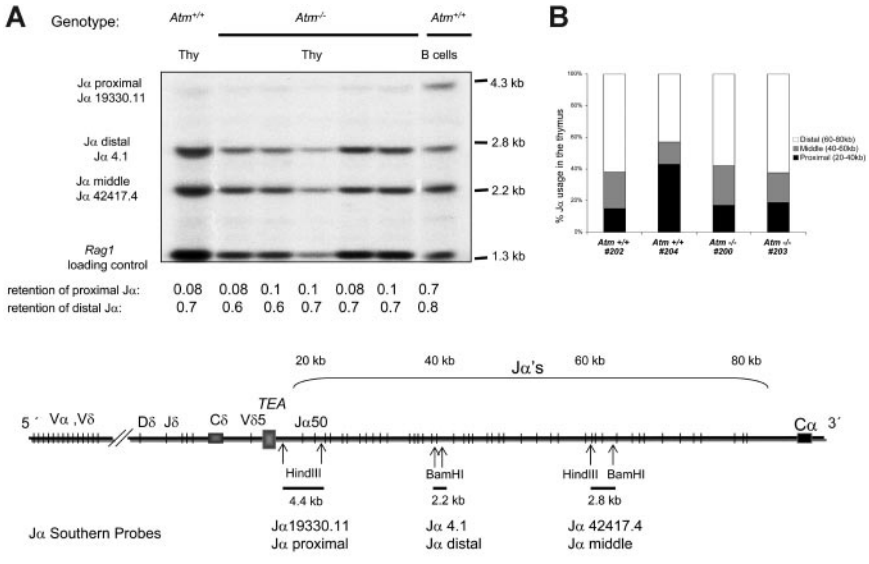

Figure 6. Analysis of secondary *Tcra* locus recombination in *Atm*$^{-/-}$ thymocytes. (A) Quantitation of *Ja* rearrangements by Southern blot. The *Ja* probes were 5′ (Jα19330.11), middle (Jα42417.4), and 3′ (Jα4.1). *Ja* hybridization to purified splenic B-cell DNA was used as a denominator to calculate the loss of *Ja* signals from thymocytes, shown below each lane. The schematic (not to scale; using the experimental strategy of Petrie et al[14]) represents the *Tcra* locus; arrows indicate relevant restriction sites, and the size of the genomic fragments to which each *Ja* probe hybridizes. A second experiment was performed with a similar outcome. (B) *Tcra* repertoire analysis in *Atm*$^{-/-}$ mice reveals unbiased *Ja* region usage. Thymic cDNA from two 3-week-old *Atm*$^{-/-}$ mice and 2 *Atm*$^{+/+}$ littermates was amplified with a *Va3*-specific primer and a *Ca* antisense primer. The PCR products were cloned and sequenced. The stacked histograms represent the percentages of *Tcra* mRNAs using *Ja* segments found in the 20-kb (kilobase) intervals that span the proximal (5′), middle, and distal (3′) regions of the *Ja* locus in *Atm*$^{-/-}$ thymocytes and controls. The results represent 15 independent *Atm*$^{-/-}$ and 15 *Atm*$^{+/+}$ thymus cDNA clones.

Downloaded from http://ashpublications.net/blood/article-pdf/109/5/1887/1478507/zh800507001887.pdf by guest on 08 June 2024

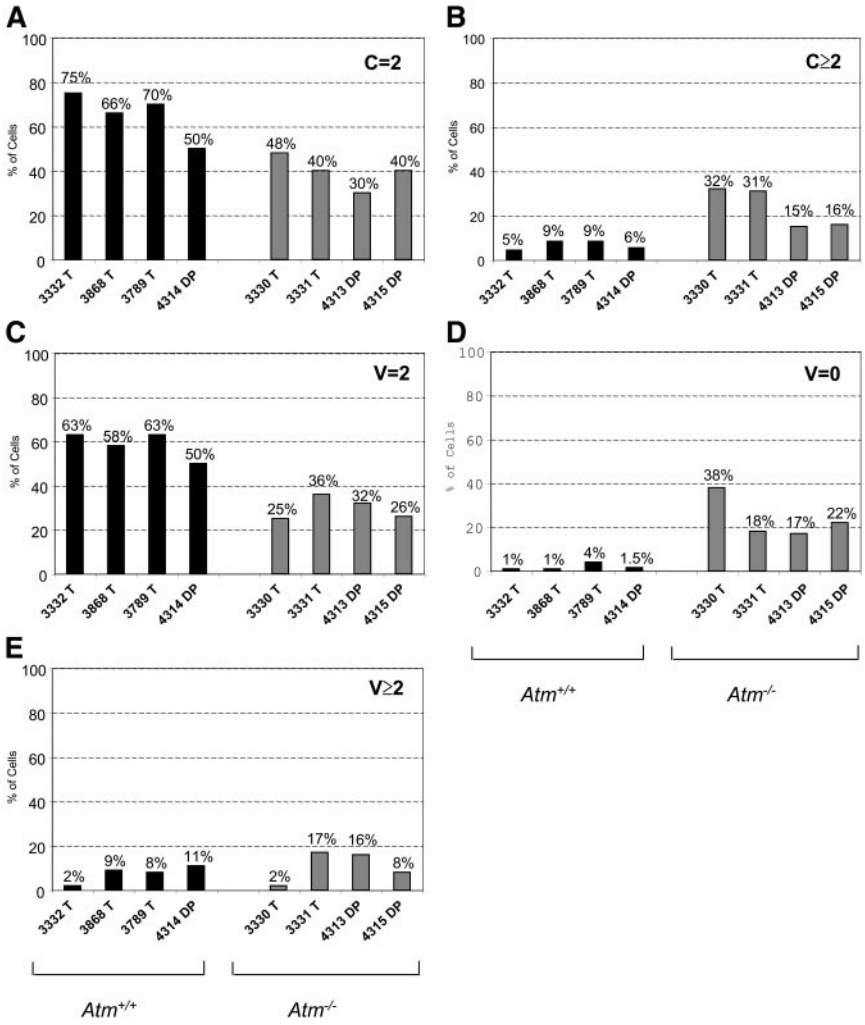

Figure 7. Biallelic *TcraV* deletions in ATM-deficient thymocytes. iFISH was performed with *TcraC* (MBAC77) and *TcraV* (MBAC01, Genebank accession AF259071) BAC probes. MBAC01 contains 6 *Va* segments located at the extreme 5′ end of the locus. Bar graphs depict the percentage of cells (vertical axis) with 0, 2, or more than 2 *TcraC* (C) or *TcraV* (V) signals per cell. For each sample 100 to 200 nuclei were imaged and scored.

the distribution of *TcraV* signals between wild-type and mutant thymocytes (Figure 7C-D). Specifically, mutant cells had frequent biallelic loss of *TcraV* signals, both in total (Figure 7D; $P < .001$; Table 1) and DP ($P < .001$) thymocytes. The iFISH images were acquired in a single plane of view potentially obscuring some signals. This technical limitation should equally affect all samples. However, we observed robust genotype-dependent differences in the numbers of *TcraV* and *TcraC* signals. Collectively, these data demonstrate that a significant proportion of $Atm^{-/-}$ thymocytes have abnormalities in the *TcraV* and *TcraC* regions. Loss of *Tcra* locus integrity in $Atm^{-/-}$ thymocytes likely underlies the developmental defect in the generation of TCR$\alpha\beta^{+}$ cells. Moreover, genomic instability at the *Tcra* locus is likely progressive during the developmental window of *Tcra* locus recombination resulting in an accumulation of abnormalities that have been reported in $Atm^{-/-}$ leukemic T cells.

Table 1. Statistical analysis of cytogenetics data

Distribution	$Atm^{+/+}$ (%)	$Atm^{-/-}$ (%)	*P*
C = 2	343 (69)	105 (45)	< .001
C ≠ 2	153 (31)	130 (55)	
C ≤ 2	455 (92)	159 (68)	< .001
C > 2	41 (8)	76 (32)	
V = 0	13 (3)	68 (29)	< .001
V ≠ 0	483 (97)	167 (71)	
V = 2	302 (61)	71 (30)	< .001
V ≠ 2	194 (39)	164 (70)	
V ≤ 2	458 (92)	215 (92)	.8
V > 2	38 (8)	20 (8)	NS

Contingency tables (2 × 2) containing the absolute numbers (and percentages) of $Atm^{+/+}$ and $Atm^{-/-}$ total thymocytes scored in each category. Thymocyte cell counts were pooled together by genotype for each category, and the probability *(P)* that the observed differences were statistically significant was determined by a standard chi-square test. The C = 0 category was omitted because thymocytes lacking both *TcraC* signals were not found in either $Atm^{+/+}$ or $Atm^{-/-}$ thymi. Note that the V ≤ 2 versus V > 2 comparison revealed no statistically significant differences between the 2 genotypes.

NS indicates not significant.

Discussion

We have demonstrated that the paucity of mature SP thymocytes in $Atm^{-/-}$ mice reflects impaired TCRα expression and defective maturation of postmitotic DP thymocytes. Surprisingly, we found no impairment of *Tcrb* recombination or generation of a diverse primary TCRβ repertoire. Furthermore, ATM loss did not compromise proliferation or survival during the DN to DP transition, because BrdU pulse-chase studies showed that normal numbers of TCRβ^{low} DP thymocytes were generated in response to pre-TCR signals. In contrast, the postmitotic generation of TCRβ^{int} DP and TCRβ^{hi} SP thymocytes was dramatically impaired, and this defect

Downloaded from http://ashpublications.net/blood/article-pdf/109/5/1887/1478507/zh800507001887.pdf by guest on 08 June 2024

was not rescued by BCL-2 overexpression. However, defective generation of these populations correlated with a high frequency of large biallelic deletions encompassing the distal *TcraV* region, as well as reduced *Tcra* mRNA and protein. Thus, our data suggest that, after exiting the cell cycle, many ATM-deficient DP thymocytes undergo aberrant *TcraV* deletion and die, limiting the pool of TCRβ^{int} DP thymocytes available for positive selection. On the basis of these findings, we propose that ATM is vital for maintenance of locus integrity during the extended developmental window of *Tcra* recombination.

There are several features that could explain why ATM deficiency disrupts *Tcra* rearrangement without obviously affecting *Tcrb* recombination. First, the *Tcra* locus is dispersed over a much larger chromosomal region than the *Tcrb* locus, and the *TcraV* region alone covers nearly 1 megabase.[30] Such long-range recombination events might be more prone to disruption in the absence of ATM. In support of this notion, ATM deficiency also impairs class-switch recombination,[45,46] another event involving rearrangements over long chromosomal distances. Second, the *Tcrd* locus, which rearranges during the DN stage of development, is contained within the *Tcra* locus on mouse chromosome 14.[30] Moreover, *Tcra* but not *Tcrb* gene segments can undergo repeated rounds of secondary recombination on the same chromosome.[12,47] Thus, chromosome 14 must remain patent during many rounds of V(D)J recombination at 2 different developmental stages. Finally, signaling through TCRβ-containing pre-TCR complexes triggers robust clonal expansion during the DN to DP transition,[35] whereas TCRαβ signaling induces DP thymocytes to mature without proliferating.[48] Thus, a reduced efficiency of *Tcrb* recombination in ATM-deficient DN thymocytes could be masked by proliferative expansion. Notably, 1 study reported that patients with AT exhibit restricted peripheral *TCR-VB* repertoires and oligoclonal CDR3 regions.[7] The distinction between that study and the data reported here likely reflects differences between primary unselected and peripheral *TCR-Vb* repertoires. Moreover, our ATM-deficient mice were housed in specific pathogen-free conditions, whereas patients with AT have recurrent sinopulmonary infections, which would likely skew an already limited peripheral TCR repertoire.

Despite normal generation of TCRβ-expressing DP precursors, the pool of postmitotic TCRβ^{int} DP thymocytes was dramatically reduced in *Atm*$^{-/-}$ mice. Surprisingly, although this reduction correlated with a striking reduction in *Tcra* expression, proximal *Ja* rearrangement and secondary *Ja* recombination were not obviously impaired in ATM-deficient thymocytes. However, these approaches did not evaluate whether these rearrangements contained normal *Va-Ja* coding joints. Because our molecular cytogenetic analyses showed frequent biallelic deletion of the entire distal *TcraV* gene cluster, it is possible that many of the *Ja* rearrangements detected by Southern blotting were aberrant. Collectively, these observations reveal that ATM plays a critical role in maintaining *Tcra* locus integrity during recombination.

Our conclusion accords with the observation that ATM localizes to RAG-induced DSBs,[22] as well as with the recent suggestion that ATM stabilizes DSB repair complexes during inversional V(D)J recombination.[29] This study used immortalized pre–B-cell lines harboring chromosomally integrated artificial V(D)J substrates to demonstrate that ATM deficiency reduces inversional recombination efficiency by 50%. We observed an even greater defect in TCRα production in ATM-deficient thymocytes in vivo, perhaps reflecting a compounded inefficiency of multiple recombination events across this large locus. The large deficit in TCRα expression in vivo could also reflect accelerated death of DP thymocytes harboring aberrant *Tcra* rearrangements, in addition to inefficient recombination.

Surprisingly, the Bredemeyer et al[29] study reported abnormal CE accumulation during rearrangement of the inversion substrate in *Atm*$^{-/-}$ pre–B-cell lines, whereas we did not observe persistence of *Ja50* CEs during deletional recombination in primary ATM-deficient thymocytes. Several possibilities could account for this apparent discrepancy. First, in the cell line model, recombination was temporally synchronized and only one CE could be generated. In contrast, *Ja* recombination occurs asynchronously in vivo, and many different *Ja* CEs can be generated across the locus. Indeed, we observed normal frequencies of middle and distal *Ja* recombination events. Thus, the concentration of particular *Ja* CEs may be too low in primary ATM-deficient thymocytes to detect by Southern blotting. Moreover, the substrate CEs were short-lived in pre-B cell lines.[29] This rapid degradation could make *Ja* CEs very difficult to detect in asynchronous populations of ATM-deficient thymocytes.

We have previously shown that the abnormal accumulation of V(D)J DSBs in NHEJ-deficient thymocytes activates the p53-mediated DNA damage response pathway.[18] Analyses of *Atm;p53* double-mutant mice have demonstrated that the p53 and ATM-dependent DNA damage response pathways are not entirely overlapping,[49-51] and ATM loss can lead to induction of p53-dependent apoptosis.[52] Indeed, spontaneous apoptosis was enhanced in ATM-deficient thymocytes (Figure S2; Elson et al[10]). Therefore, we examined whether an antiapoptotic *Bcl2* transgene would rescue the *Atm* null phenotype. Although BCL-2 overexpression in *Atm*$^{-/-}$ mice generally enhanced lymphocyte survival and thymic cellularity, it failed to rescue maturation of TCRβ^{int} DP thymocytes from TCRβ^{low} precursors. Therefore, impaired maturation of ATM-deficient thymocytes does not reflect activation of a BCL-2–sensitive apoptotic pathway.

In summary, our study provides a molecular and developmental explanation for the T-cell immune deficiency that is characteristic of patients with AT and ATM-deficient mice. In contrast to NHEJ deficiencies which cause profound failure of *Tcrb* and *Tcra* recombination,[16,43] we showed that ATM loss results in decreased *Tcra* expression, resulting in a paucity of TCRαβ heterodimer. Nonetheless, this defect is sufficient to profoundly impair maturation and positive selection of *Atm*$^{-/-}$ DP thymocytes. Our molecular cytogenetic analyses strongly suggest that aberrant *Tcra* recombination underlies these defects, and we propose that ATM maintains locus integrity as DP thymocytes make multiple attempts to successfully recombine *Tcra*. However, thymocytes can partially compensate for ATM loss, perhaps at the cost of genomic stability. The high incidence of T-cell leukemias/lymphomas bearing *Tcra* locus alterations in *Atm*$^{-/-}$ mice and patients with AT supports the hypothesis that some ATM-deficient thymocytes escape apoptotic pathways that normally eliminate cells harboring DNA damage.

Acknowledgments

We thank Dr S. Zhao for expert flow cytometry, the late Dr S. Korsmeyer for providing the *lckpr-BCL2* transgenic mice, and Drs H. Petrie and F. Livak for sharing the *Ja* plasmids and probes. We thank Drs Vikram Jayanth and Martin Lee from The Centre for Applied Genomics (Hospital for Sick Children Research Institute) for performing the iFISH experiments. We also thank Dr Inoul Lee (University of Washington, Seattle) for BAC clones and I. Grandal and C. Webb for animal care.

This work was supported by grants from the Leukemia and Lymphoma Society (J.S.D. and C.J.G.), Genome Canada (J.S.D. and C.J.G.), and the Ontario Genomics Institute (J.S.D. and C.J.G.). R.A.G.

Downloaded from http://ashpublications.net/blood/article-pdf/109/5/1887/1478507/zh800507001887.pdf by guest on 08 June 2024

held Canadian Institutes of Health Research (CIHR) and National Cancer Institute of Canada (NCIC) Fellowship awards. I.R.M. was supported by a RESTRACOMP Studentship from the Hospital for Sick Children Research Institute.

Authorship

Contribution: I.R.M. performed most of the research, analyzed the data, and cowrote the paper; R.A.G. performed some experiments and analyzed the data; L.M.J.N. contributed to the design of the study and supervised the experimental work; A.C. designed and performed the statistical analysis of the cytogenetics data; C.J.G. and J.S.D. designed the study, supervised the experimental work, and cowrote the manuscript.

Conflict-of-interest disclosure: The authors declare no competing financial interests.

Correspondence: Jayne S. Danska, The Hospital for Sick Children Research Institute, 101 College St, Toronto Medical Discovery Tower (TMDT) East Tower, Rm 14-313, Toronto, ON M5G 1L7 Canada; e-mail: jayne.danska@sickkids.ca.

References

1. Taylor AMR, Metcalfe Ja, Mak YF. Leukemia and lymphoma in ataxia telangiectasia. Blood. 1996; 87:423-438.
2. Shiloh Y. ATM and related protein kinases: safeguarding genome integrity. Nat Rev Cancer. 2003;3:155-168.
3. Xu Y, Ashley T, Brainerd EE, Bronson RT, Meyn MS, Baltimore D. Targeted disruption of ATM leads to growth retardation, chromosomal fragmentation during meiosis, immune defects, and thymic lymphoma. Genes Dev. 1996;10:2411-2422.
4. Morrison C, Sonoda E, Takao N, Shinohara A, Yamamoto K, Takeda S. The controlling role of ATM in homologous recombinational repair of DNA damage. EMBO J. 2000;19:463-471.
5. Barlow C, Liyanage M, Moens PB, et al. Atm deficiency results in severe meiotic disruption as early as leptonema of prophase I. Development. 1998;125:4007-4017.
6. Waldman TA. Immunological abnormalities in ataxia-telangiectasia. In: Bridges BA, Harnden DG, eds. Ataxia-telangiectasia: A Cellular and Molecular Link between Cancer, Neuropathology and Immune Deficiency. New York, NY: John Wiley and Sons; 1982:37-52.
7. Giovannetti A, Mazzetta F, Caprini E, et al. Skewed T-cell receptor repertoire, decreased thymic output, and predominance of terminally differentiated T cells in ataxia telangiectasia. Blood. 2002;100:4082-4089.
8. Barlow C, Hirotsune S, Paylor R, et al. Atm-deficient mice: a paradigm of ataxia telangiectasia. Cell. 1996;86:159-171.
9. Xu Y, Baltimore D. Dual roles of ATM in the cellular response to radiation and in cell growth control. Genes Dev. 1996;10:2401-2410.
10. Elson A, Wang Y, Daugherty CJ, et al. Pleiotropic defects in ataxia-telangiectasia protein-deficient mice. Proc Natl Acad Sci U S A. 1996;93:13084-13089.
11. Borghesani PR, Alt FW, Bottaro A, et al. Abnormal development of Purkinje cells and lymphocytes in Atm mutant mice. Proc Natl Acad Sci U S A. 2000;97:3336-3341.
12. Krangel MS, Carabana J, Abbarategui I, Schlimgen R, Hawwari A. Enforcing order within a complex locus: current perspectives on the control of V(D)J recombination at the murine T-cell receptor alpha/delta locus. Immunol Rev. 2004;200:224-232.
13. Petrie HT, Livak F, Schatz DG, Strasser A, Crispe IN, Shortman K. Multiple rearrangements in T cell receptor alpha chain genes maximize the production of useful thymocytes. J Exp Med. 1993;178: 615-622.
14. Petrie HT, Livak F, Burtrum D, Mazel S. T cell receptor gene recombination patterns and mechanisms: cell death, rescue, and T cell production. J Exp Med. 1995;182:121-127.
15. Yannoutsos N, Wilson P, Yu W, et al. The role of recombination activating gene (RAG) reinduction in thymocyte development in vivo. J Exp Med. 2001;194:471-480.
16. Rooney S, Chaudhuri J, Alt FW. The role of the non-homologous end-joining pathway in lymphocyte development. Immunol Rev. 2004;200:115-131.
17. Roth D, Menetski J, Nakajima P, Bosma M, Gellert M. V(D)J recombination: broken DNA molecules with covalently sealed (hairpin) coding ends in scid mouse thymocytes. Cell. 1992;70: 983-991.
18. Guidos CJ, Williams CJ, Grandal I, Knowles G, Huang MT, Danska JS. V(D)J recombination activates a p53-dependent DNA damage checkpoint in scid lymphocyte precursors. Genes Dev. 1996; 10:2038-2054.
19. Difilippantonio MJ, Zhu J, Chen HT, et al. DNA repair protein Ku80 suppresses chromosomal aberrations and malignant transformation. Nature. 2000;404:510-514.
20. Zhu C, Mills KD, Ferguson DO, et al. Unrepaired DNA breaks in p53-deficient cells lead to oncogenic gene amplification subsequent to translocations. Cell. 2002;109:811-821.
21. Gladdy RA, Taylor MD, Williams CJ, et al. The RAG-1/2 endonuclease causes genomic instability and controls CNS complications of lymphoblastic leukemia in p53/Prkdc-deficient mice. Cancer Cell. 2003;3:37-50.
22. Perkins EJ, Nair A, Cowley DO, Van Dyke T, Chang Y, Ramsden DA. Sensing of intermediates in V(D)J recombination by ATM. Genes Dev. 2002;16:159-164.
23. Chen HT, Bhandoola A, Difilippantonio MJ, et al. Response to RAG-mediated VDJ cleavage by NBS1 and gamma-H2AX. Science. 2000;290: 1962-1965.
24. Celeste A, Petersen S, Romanienko PJ, et al. Genomic instability in mice lacking histone H2AX. Science. 2002;296:922-927.
25. Difilippantonio S, Celeste A, Fernandez-Capetillo O, et al. Role of Nbs1 in the activation of the Atm kinase revealed in humanized mouse models. Nat Cell Biol. 2005;7:675-685.
26. Liyanage M, Weaver Z, Barlow C, et al. Abnormal rearrangement within the alpha/delta T-cell receptor locus in lymphomas from Atm-deficient mice. Blood. 2000;96:1940-1946.
27. Lipkowitz S, Stern M-H, Kirsch IR. Hybrid T cell receptor genes formed by interlocus recombination in normal and ataxia-telangiectasia lymphocytes. J Exp Med. 1990;172:409-418.
28. Lista F, Bertness V, Guidos CJ, Danska JS, Kirsch IR. The absolute number of trans-rearrangements between the TCRG and Tcrb loci is predictive of lymphoma risk: a severe combined immune deficiency (SCID) murine model. Cancer Res. 1997;57:4408-4413.
29. Bredemeyer AL, Sharma GG, Huang CY, et al. ATM stabilizes DNA double-strand-break complexes during V(D)J recombination. Nature. 2006; 442:466-470.
30. Glusman G, Rowen L, Lee I, et al. Comparative genomics of the human and mouse T cell receptor loci. Immunity. 2001;15:337-349.
31. Sentman CL, Shutter JR, Hockenbery D, Kanagawa O, Korsmeyer SJ. bcl-2 inhibits multiple forms of apoptosis but not negative selection in thymocytes. Cell. 1991;67:879-888.
32. Danska JS, Holland DP, Mariathasan S, Williams KM, Guidos CJ. Biochemical and genetic defects in the DNA-dependent protein kinase in murine scid lymphocytes. Mol Cell Biol. 1996;16:5507-5517.
33. Groves T, Parsons M, Miyamoto NG, Guidos CJ. TCR engagement of CD4+CD8+ thymocytes in vitro induces early aspects of positive selection, but not apoptosis. J Immunol. 1997; 158:65-75.
34. Guidos CJ. Positive selection of CD4+ and CD8+ T cells. Curr Opin Immunol. 1996;8:225-232.
35. von Boehmer H. Unique features of the pre-T-cell receptor alpha-chain: not just a surrogate. Nat Rev Immunol. 2005;5:571-577.
36. Lucas B, Vasseur F, Penit C. Normal sequence of phenotypic transitions in one cohort of 5-bromo-2'-deoxyuridine-pulse-labeled thymocytes. Correlation with T cell receptor expression. J Immunol. 1993;151:4574-4582.
37. Surh CD, Sprent J. T-cell apoptosis detected in situ during positive and negative selection in the thymus. Nature. 1994;372:100-103.
38. Guo J, Hawwari A, Li H, et al. Regulation of the TCRalpha repertoire by the survival window of CD4(+)CD8(+) thymocytes. Nat Immunol. 2002; 3:469-476.
39. Morse HC III, Anver MR, Fredrickson TN, et al. Bethesda proposals for classification of lymphoid neoplasms in mice. Blood. 2002;100:246-258.
40. Kappler JW, Kushnir E, Marrack P. Analysis of V beta 17a expression in new mouse strains bearing the V beta a haplotype. J Exp Med. 1989;169: 1533-1541.
41. Kearse KP, Roberts JP, Wiest DL, Singer A. Developmental regulation of alpha beta T cell antigen receptor assembly in immature CD4+CD8+ thymocytes. Bioessays. 1995;17: 1049-1054.
42. Livak F, Schatz DG. T cell receptor α locus V(D)J recombination by-products are abundant in thymocytes and mature T cells. Mol Cell Biol. 1996; 16:609-618.
43. Livak F, Welsh SC, Guidos CJ, Crispe IN, Danska JS, Schatz DG. Transient restoration of gene rearrangement at multiple T cell receptor loci in gamma-irradiated scid mice. J Exp Med. 1996; 184:419-428.
44. Taylor AM, Metcalfe Ja, Thick J, Mak YF. Leukemia and lymphoma in ataxia telangiectasia. Blood. 1996;87:423-438.
45. Lumsden JM, McCarty T, Petiniot LK, et al. Immunoglobulin class switch recombination is impaired

Downloaded from http://ashpublications.net/blood/article-pdf/109/5/1887/1478507/zh800507001887.pdf by guest on 08 June 2024

in Atm-deficient mice. J Exp Med. 2004;200:1111-1121.

46. Reina-San-Martin B, Chen HT, Nussenzweig A, Nussenzweig MC. ATM is required for efficient recombination between immunoglobulin switch regions. J Exp Med. 2004;200:1103-1110.
47. Jackson AM, Krangel MS. Turning T-cell receptor beta recombination on and off: more questions than answers. Immunol Rev. 2006;209:129-141.
48. Huesmann M, Scott B, Kisielow P, von Boehmer H. Kinetics and efficacy of positive selection in the thymus of normal and T cell receptor transgenic mice. Cell. 1991;66:533-540.
49. Westphal CH, Rowan S, Schmaltz C, Elson A, Fisher DE, Leder P. atm and p53 cooperate in apoptosis and suppression of tumorigenesis, but not in resistance to acute radiation toxicity. Nat Genet. 1997;16:397-401.
50. Westphal CH, Schmaltz C, Rowan S, Elson A, Fisher DE, Leder P. Genetic interactions between atm and p53 influence cellular proliferation and irradiation-induced cell cycle checkpoints. Cancer Res. 1997;57:1664-1667.
51. Barlow C, Brown KD, Deng CX, Tagle DA, Wynshaw-Boris A. Atm selectively regulates distinct p53-dependent cell-cycle checkpoint and apoptotic pathways [published erratum appears in Nat Genet. 1998;18:298]. Nat Genet. 1997;17:453-456.
52. Barlow C, Liyanage M, Moens PB, Deng CX, Ried T, Wynshaw-Boris A. Partial rescue of the prophase I defects of Atm-deficient mice by p53 and p21 null alleles. Nat Genet. 1997;17:462-466.

Downloaded from http://ashpublications.net/blood/article-pdf/109/5/1887/1478507/zh800507001887.pdf by guest on 08 June 2024